

Freeze-out of the Fireball

David H. Boal
Department of Physics
Simon Fraser University
Burnaby, B.C., Canada V5A 1S6

I. Introduction

There is ample evidence¹ that multiple scattering of nucleons plays an important role in the emission of energetic particles in nuclear reactions,² and may lead to a system of particles which is in thermal, and perhaps even chemical equilibrium. In the past, a significant amount of effort has gone into determining how, or even if, such an equilibrated system can be formed. Yet it is equally important to know the time evolution of the system through to when the participants go out of thermal equilibrium.³ In this lecture, attention will be focussed on the last stage of the evolution of the nuclear fireball: freeze-out.

One can get a theoretical estimate of the time scale for the evolution of a hot, equilibrated region of nuclear matter from the following considerations: Imagine that a projectile has created an equilibrated region in a large target nucleus. The classical diffusion equation

$$\frac{\partial T(r,t)}{\partial t} = \frac{1}{C_p} \operatorname{div} \left(\frac{\kappa}{\rho} \operatorname{grad} T(r,t) \right) \quad (1)$$

can be used to follow the evolution of the temperature T as a function of space and time. In Eq. (1) κ is the thermal conductivity, ρ the density and C_p the specific heat. The results of such a calculation (see Ref. 2 for details) are shown in Fig. 1 for a gaussian spatial distribution of the initial temperature

$$T(r,0) = \exp(-r^2/r_0^2) \quad (2)$$

where r_0 has been chosen to be 3 fm. Figure 1a shows an estimate of the rate of change of the temperature in the centre of the hot region, while Fig. 1b shows an estimate of the time scale involved, found by

dividing the central temperature by its rate of change. One sees that time scales on the order of a few times 10^{-23} sec are indicated in this calculation.

Of course, one wants to be able to obtain experimental information on what time scales are involved. Two approaches will be outlined here. In the first, one finds a quantity whose time evolution can be both calculated and measured. One such example is the proton to neutron ratio of the equilibrated region in proton or muon induced reactions.⁴ In free μ^- capture, only energetic neutrons are produced. One can calculate the time rate of change of the p/n ratio in this reaction as it changes from zero initially to Z/N of the target if it evolves to its chemical equilibrium value (neglecting binding energy effects). Experimentally, this ratio is observed to be far from its chemical equilibrium value and a time of the order 10^{-23} sec is indicated for the lifetime of the hot region. The evolution of other chemical abundances will be discussed below. This approach has also been applied to systems with much higher temperatures than those considered here by considering the K^+/K^- ratio.⁵

A second approach is to use the technique of nuclear interferometry.⁶ Experimentally, a correlation function defined by

$$c(\vec{p}_1, \vec{p}_2) = \sigma \frac{d^6\sigma/d^3p_1 d^3p_2}{(d^3\sigma/d^3p_1)(d^3\sigma/d^3p_2)} - 1 \quad (3)$$

is measured at momenta \vec{p}_1 and \vec{p}_2 small relative to each other. This technique has been widely applied to both two-pion and two-proton interferometry. Taking a low energy heavy ion reaction as an example, the two-proton correlation function measured⁷ in a reaction involving 25 MeV/nucleon ^{16}O on Au is shown in Fig. 2 along with a calculation⁸ of the correlation function expected for a gaussian (in space) source of nucleons with width parameter r_0 .

One can see that a value of 3.5-4 fm is indicated for r_0 . Although this number looks small, it should be remembered that a uniform density distribution would have a radius $\sqrt{\frac{5}{2}} r_0$ if it were to have the same rms radius ($\sqrt{\frac{3}{2}} r_0$) as the gaussian.

Recent work^{9,10} has extended this approach to two-deuteron, two triton and other particle correlations. This opens up the possibility that one can follow the spatial expansion of the fireball, since each of the particle species have different cross sections and would be expected to go out of thermal equilibrium at different times. An example of the two-deuteron and two-triton correlations is shown in Fig. 3. The theoretical curves show the results obtained using coulomb phase shifts alone, as well as two different sets of phase shifts for the dd nuclear interaction. The R-matrix (RM) results¹¹ are the more complete in the energy range required here, and are clearly favoured by the data over the phase shifts found using the resonating group (RG) approach.¹² Substantially larger source sizes are found for deuterons and tritons, about 50% larger than those found for protons. Similar results have been found¹³ in an analysis of the higher energy (400 A·MeV Ca+Ca) data reported in Ref. 9.

III. A Model for Freeze-out

In energetic heavy ion reactions, the energetic particles measured in the experiments which we have been discussing, appear to come from a source which has a velocity distinct from that of the projectile or target remnants. It may be possible to imagine the expansion and cooling of this interaction region without concerning oneself about its interaction with the other blobs of cold matter.

Let us construct a model for the expansion phase. It will be assumed that by the time the initial thermalization step of the reaction is over, the hot fireball which it produced has no large scale inhomogeneities and has a density of about nuclear matter. As the system evolves, both the initial temperature T_0 which characterizes the system and the density ρ will decrease. It will be assumed, therefore, that in the expansion phase three-body interactions can be neglected, an assumption which improves as freeze-out is approached. For convenience, the participant nucleons will be uniformly distributed in a spherical volume. The time evolution of this system is then followed in the cascade model sense: a Monte Carlo initialization of the system is made and then the trajectories of the nucleons are computed using

relativistic mechanics but ignoring quantum effects. Typically 200 or more such events are averaged over to obtain reasonable statistics.

To compare the results of this model with experiment, we first estimate the freeze-out density by finding the time at which the average reaction time τ_{rxn} exceeds the expansion time, τ_{exp} , of the system. The reaction time is obtained simply by counting the number of NN collisions in a particular time bin. The characteristic expansion time of the system is defined here by

$$\tau_{\text{exp}} = \langle r^2 \rangle^{1/2} / (d \langle r^2 \rangle^{1/2} / dt) \quad (4)$$

One can use the rms radius obtained at freeze-out to make a comparison with the two particle correlation results, as is shown in Fig. 4. The experimental data¹⁴ are from Ca+Ca collisions at 400 A·MeV, and the source parameter is shown as a function of charged particle multiplicity. For the theoretical curve, it has been assumed that the number of nucleons in the source is double the charged particle multiplicity. The value of r_0 obtained from the model is that of a gaussian distribution with the same r.m.s. radius as that found numerically:

$r_0 = \sqrt{\frac{2}{3}} r_{\text{rms}}$. One can see that the agreement is at least qualitative. If one corrects for the finite lifetime of the source ($\tau=0$ for the data analysis shown in Fig. 4) then r_0 obtained experimentally, will decrease. For example,¹³ assuming a lifetime of 5×10^{-23} sec will decrease the experimental value of r_0 by 0.4 to 0.6 fm. One can estimate the freeze-out densities for deuterons and tritons in a similar fashion. The model shows an increase in the value of r_0 (5 fm for deuterons, 6-7 fm for tritons) over the proton results of about 50% for these nuclei, as is found experimentally.

As the system expands, the temperature (as measured in a co-moving frame) decreases. Shown in Fig. 5 is the behaviour of the temperature in the central region ($r < 2$ fm) of the fireball as a function of time. The approximate freeze-out times for several species are indicated. This decrease in the local temperature does not necessarily imply a shift in the energy spectrum. For example, if we started with a fixed number of particles forming an ideal gas, then conservation of energy would imply that the average energy per particle remain constant.

What should change, however, is the relative abundance of particle species. So long as a species remains in chemical equilibrium, its abundance relative to other species will be determined by the local temperature. Hence, excited state populations, or the abundance of certain nuclei which are less well bound than others, should decrease with increasing time until freeze-out of the species involved. In addition to using two particle correlations, then, to determine freeze-out parameters, one could also use the chemical abundances of various nuclear species.

An experiment which may be an example of this effect was recently performed¹⁵ with a reaction involving 35 A·MeV $^{14}\text{N} + \text{Ag}$. In this experiment, the first excited state to ground state population ratio was measured for ^6Li , ^7Li and ^7Be reaction products. The population ratios showed temperatures of 1/2 to 1 MeV, in contrast to 9 MeV found by analysing the differential cross section with a moving source model. A calculation of the freeze-out point for Li fragments in this experiment has been performed using similar methods to those outlined above, except that an analytic expression for the local temperature was used (see Ref. 16 for details). The calculation is shown in Fig. 6. In this calculation, the excited state to ground state reaction goes out of equilibrium at a temperature of 0.6 MeV, corresponding to an elapsed time of 2×10^{-22} sec and a freeze-out density of 1/20 normal nuclear matter density.

To summarize, the cascade model presented here can be used to obtain source dimensions as well as freeze-out densities and temperatures. The predictions agree with the existing two particle correlation data, as well as freeze-out temperatures obtained from excited state population ratio arguments. The model will now be applied to the formation of intermediate mass fragments.

IV. Fragment Production

The fact that the thermal model description of heavy ion reactions has been so successful has led to the investigation of the critical properties of nuclear matter and the search for phase transitions. One of the crucial problems in the study of the liquid-gas phase transition has been whether the reaction products are still

in equilibrium by the time they reach the phase transition region, and whether there is sufficient time for the transition to occur. Progress in understanding the time scales for nuclear reactions will help unravel these questions.

Shown in Fig. 7 is a calculation of the liquid-gas coexistence region.¹⁷ One can imagine two very different approaches to this region which may show phase transition effects. These are illustrated in Fig. 8. If the system is very hot as it starts the expansion phase, then the reaction path might pass fairly close to the critical region. One might expect to see phenomena such as liquid droplet formation from the hadronic vapour.¹⁸ A different path would involve systems with low initial temperatures. Then the phenomena of fragment formation is more like bubble growth,¹⁹ as illustrated in Fig. 8b. Our cascade model is unlikely to be of use in this region, since Pauli blocking and many other effects are bound to be important.

Returning to the high temperature region, then, the trajectory followed by an expanding gas of Maxwell-Boltzmann nucleons with an initial temperature of 25 MeV is shown in Fig. 7. [The calculation follows Refs. 16,20; see Eqs. (5)-(7) below. This approach is shown, rather than the cascade calculation since the statistics of the latter were not as good as one would like, although at no point did the results deviate by more than 20% from the curve shown.] The freeze-out point is rather difficult to estimate, since it will depend on the various particle species involved, and what reactions keep them in equilibrium. For example, the lithium excited state to ground state reaction examined in the last section has a large cross section since it can go via an (n,n') reaction. In contrast, ${}^7\text{Be} \leftrightarrow {}^7\text{Li}$ will involve a charged proton tunnelling through the coulomb barrier, and so would have a much smaller cross section at temperatures of a few MeV. This conclusion would be even stronger for heavier fragments: their freeze-out densities may be substantially larger than that found for Li. An educated guess might put freeze-out at $1/10 \rho_0$, subject to large uncertainties.

If freeze-out does occur in the coexistence region, then one may be able to apply statistical ideas to quantities such as the fragment

yield curves. This approach has been taken by many authors and has yielded good (one parameter) fits to the data.¹⁸ However, this should not necessarily be interpreted as meaning that there is a sharp change of phase between a nucleon gas and a mixture of gas and droplets (to use the language appropriate to the high temperature part of the phase diagram). One can show that the time scale associated with the build-up of fragments from the nucleon gas is comparable to that of the lifetime of the system by examining the reaction rates involved.^{21,22}

In Ref. 21, a simplified set of rate equations were solved for the time evolution of a system initially composed of nucleons to approach chemical equilibrium. The processes considered were all two-body, so the model will not be applicable in the low temperature high density regime. The results which we wish to present here involve some modifications of Ref. 21. First, rather than choose fixed values of the temperature and density at which the rates are evaluated, we calculate the evolution of small volume elements of a system expanding according to^{20,16}

$$T(t) = T_0 \gamma \quad (5)$$

$$\rho(\vec{r}, t) = A \left(\frac{\gamma}{2\pi\Delta^2} \right)^{3/2} e^{-\gamma r^2/2\Delta^2} \quad (6)$$

where

$$\gamma = (1 + T_0 t^2/m\Delta^2)^{-1} \quad (7)$$

The parameter Δ was fixed as $1.2 A^{1/3}/\sqrt{5}$ fm with $A = 50$. The yields were determined by numerically integrating over all volume elements. In addition, a breakup reaction $N+A \rightarrow N+N+(A-1)$ was introduced to complement the two body fusion processes. The results of the calculation are shown in Fig. 9.

What has been plotted is the behaviour of the exponent τ when the fragment yields are parametrized as

$$Y(A) \propto A_F^{-\tau} \quad (8)$$

for $10 < A_F < 20$, A_F being the mass number of the fragment. One can see that the system is mainly nucleons near $t=0$ (i.e., τ is large), and that the fragment abundances increase as a function of time. The values of τ which are obtained by analysing the experimental mass yield

curves are typically in the 2 to 4 range, and one can see that the rate equations lead to these values as well. However, in contrast to the phase transition model, in which these values of τ are a result of statistics, here τ is a result of dynamics. Further, the "asymptotic" values of τ reached in Fig. 9 are a result of the system going out of equilibrium, and not a result of the system achieving chemical equilibrium.²³ Inclusion of coulomb effects²⁴ will lead to an earlier freeze-out of the $T_0 = 15$ MeV results than is indicated on the figure.

V. Conclusion

It has been shown that the linear dimension of the emitting region for deuterons and tritons is about 50% larger than is found for protons in an analysis of two-particle correlation measurements in heavy ion reactions. This suggests that there may be a sequential freeze-out of various nuclear species, nuclei with larger cross sections going out of equilibrium later than those with smaller cross sections. This hypothesis is also supported by the measurements of the excited state to ground state population ratios of ${}^6\text{Li}$, ${}^7\text{Li}$ and ${}^7\text{Be}$. A cascade model was presented which allowed an estimate of the freeze-out densities and temperatures to be made for light nuclei in the low density regimes and these estimates were shown to be consistent with the experimental results.

This model was then used to find the trajectory of the expansion regime in the T, ρ plane, in particular to see in what part of the phase transition regime it lay. It was shown by means of a coupled set of rate equations that, in the time scale indicated by the cascade results ($1-2 \times 10^{-22}$ sec), light nuclear fragments could be built up from a nucleon gas in the abundances indicated by experiment. However, the time scale indicated would imply that there is not a sharp transition between an exclusively nucleon phase and the observed fragment distribution. This does not mean that statistics do not play an important role in determining the mass yield distribution. The answer to that question lies in how fast the species can re-equilibrate as the system expands. It also does not mean that the initial system can be well described as being a uniform distribution of nucleons. Indeed, there will be substantial fluctuations present from the thermalization phase

and from the statistics of a relatively small number of nucleons in the reaction region. These rate calculations only indicate that variation in the chemical abundances in addition to those already present can build up on the few times 10^{-23} sec time scale.

Acknowledgement

This work was supported in part by the Natural Sciences and Engineering Research Council of Canada.

References

1. For a review of the thermal model see S. das Gupta and A.Z. Mekjian, Phys. Rep. 72, 131 (1981).
2. For a review of energetic particle emission, see D.H. Boal in Advances in Nuclear Physics, J.W. Negele and E. Vogt, eds. (Plenum, New York, in press).
3. For several different approaches to this problem, see, for example, H. Stöcker, J. Hofmann, J.A. Maruhn and W. Greiner, Prog. Part. Nucl. Phys. 4, 133 (1980); N. Stelte and R. Weiner, University of Marburg Report (1984).
4. D.H. Boal, Phys. Rev. C29, 967 (1984).
5. A.Z. Mekjian, Nucl. Phys. A384, 492 (1982).
6. For applications in nuclear physics, see S.E. Koonin, Phys. Lett. 70B, 43 (1977); F.B. Yano and S.E. Koonin, Phys. Lett. 78B, 556 (1978).
7. W.G. Lynch et al., Phys. Rev. Lett. 51, 1850 (1983).
8. J.C. Shillcock, M.Sc. Thesis, Simon Fraser University (1984).
9. C.B. Chitwood et al., Michigan State University Report (1984).
10. H. Wieman, these proceedings.
11. G.M. Hale and B.C. Dodder, "Few-Body Problems in Physics, Vol. II", B. Zeitnitz, ed. (Elsevier, Amsterdam 1984).
12. F.S. Chwieroth et al., Nucl. Phys. A189, 1 (1972).
13. D.H. Boal and J.C. Shillcock, to be published.
14. H.A. Gustafsson et al., Phys. Rev. Lett. 53, 544 (1984).

15. D.J. Morrissey, W. Benenson, E. Kashy, B. Sherrill, A.D. Panagiotou, R.A. Blue, R.M. Ronningen, J. van der Plicht and H. Utsonomiya, Michigan State University Report No. MSUCL-454 (to be published).
16. D.H. Boal, Phys. Rev. C30, 749 (1984).
17. A.L. Goodman, J.I. Kapusta and A.Z. Mekjian, Phys. Rev. C30, 851 (1984).
18. This is the approach emphasized in Ref. 17. The reader is directed to the literature quoted in Refs. 17 and 2 for an overview of the work following this approach. See also A.L. Goodman, these proceedings.
19. See H. Reinhardt, these proceedings, as well as H. Reinhardt and H. Schulz, Nucl. Phys. A (in press).
20. J. Aichelin, Nucl. Phys. A411, 474 (1983).
21. D.H. Boal, Phys. Rev. C28, 2568 (1983).
22. For a rate equation approach to light nuclei production, see A.Z. Mekjian, Nucl. Phys. A312, 491 (1978).
23. Even higher freeze-out densities would be found using the rate equation approach of J.A. Lopez and P.J. Siemens, Texas A&M University Report (1984).
24. For several views on the role of coulomb effects on fragment yields, see D.H.E. Gross, these proceedings, as well as D.H. Boal, Phys. Rev. C30, 119 (1984).

Figure Captions

1. (a) Estimated rate of change of the central temperature of a gaussian source region in nuclear matter. b) Central temperature divided by rate of change. From Ref. 2.
2. Two-proton correlation functions measured⁶ in a 25 MeV/nucleon $^{16}\text{O} + \text{Au}$ reaction. Theoretical curves⁸ for several different gaussian source parameters are shown for comparison. From Ref. 7.
3. Two-deuteron and two-triton correlation functions for 25 MeV/nucleon ^{16}O on Au. The theoretical curves show the results for several different sets of phase shifts: resonating group (RG) and R-matrix (RM) results for the nuclear parts of the dd phase shifts as well as coulomb phase shifts with no nuclear part for both dd and tt. From Ref. 9.
4. Comparison of source parameter r_0 obtained in 400 A·MeV Ca+Ca collisions with the model calculation. For simplicity, it has been assumed that the total multiplicity is double the charged particle multiplicity obtained experimentally. The experimental results are obtained by an analysis in which the source lifetime is put equal to zero, while the model has a finite source lifetime.
5. Model calculation of the temperature in the region $r \leq 2$ fm for a 30 nucleon system shown as a function of time. The estimated freeze-out times are indicated for several particle species.
6. Calculated reaction and expansion times for the ^7Li excited state to ground state transition. The reaction goes out of equilibrium at a temperature of ~ 0.6 MeV, corresponding to an elapsed time of 2×10^{-22} sec and a central density (in this calculation) of $1/20$ nuclear matter density. (From Ref. 16).
7. Liquid-gas phase transition region (from Ref. 17) and an estimated reaction path for a system with an initial temperature of 25 MeV. The particles obey Maxwell-Boltzmann statistics in these calculations. The elapsed time during the expansion phase is also indicated.
8. Fragment formation as seen as a result of droplet formation or bubble growth.
9. Behaviour of the exponent τ of the mass yield curves as predicted by the rate equations as a function of time.

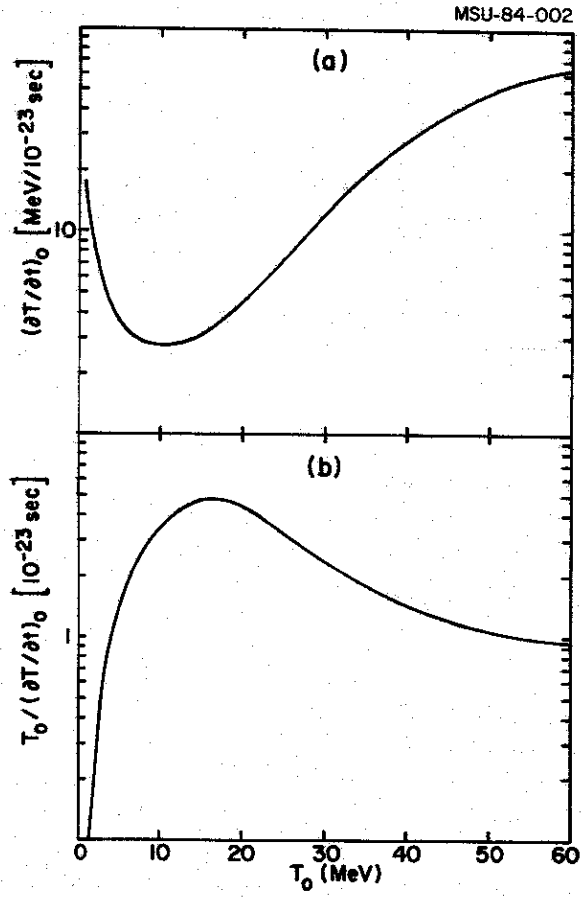


Fig. 1

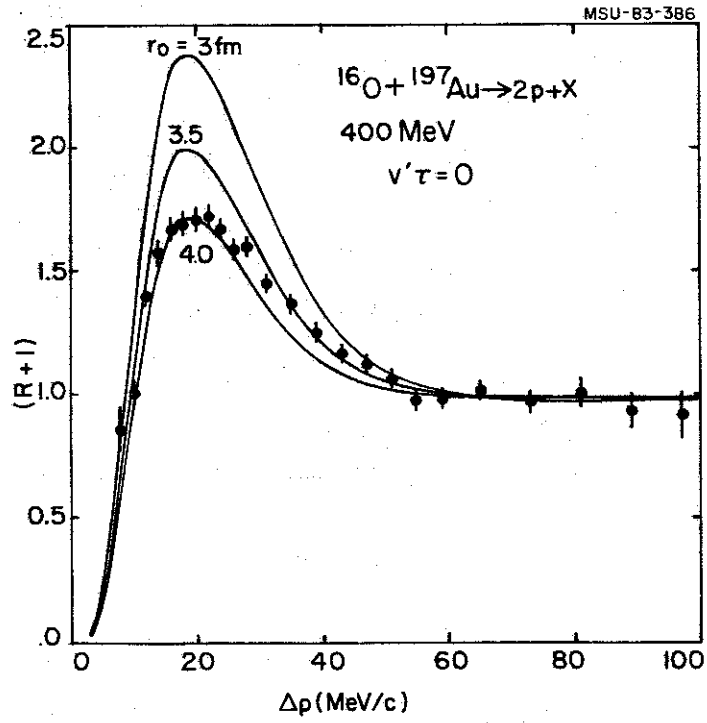


Fig. 2

MSU-84-382

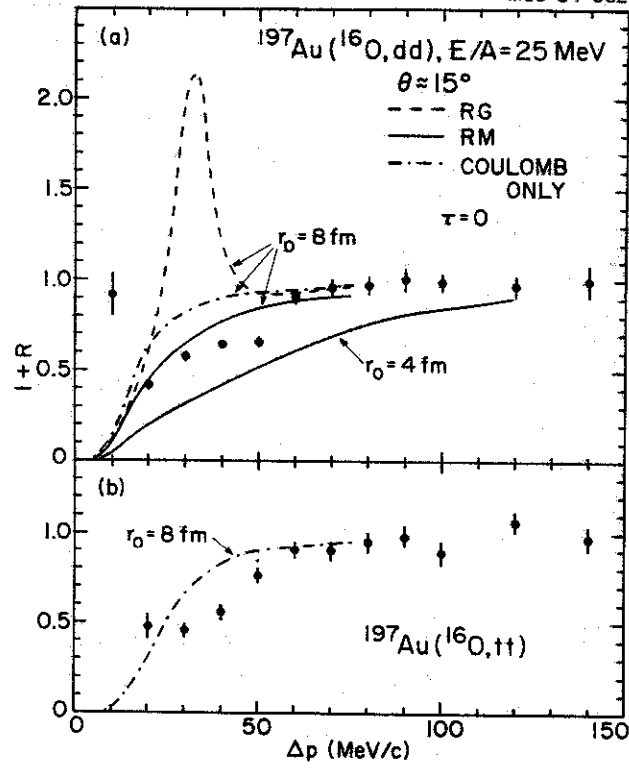


Fig. 3

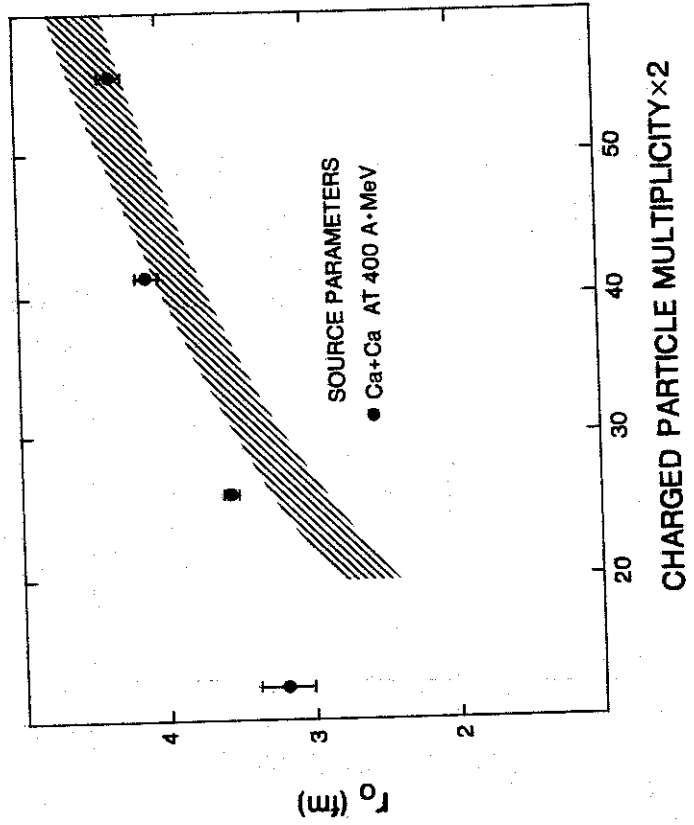


Fig. 4

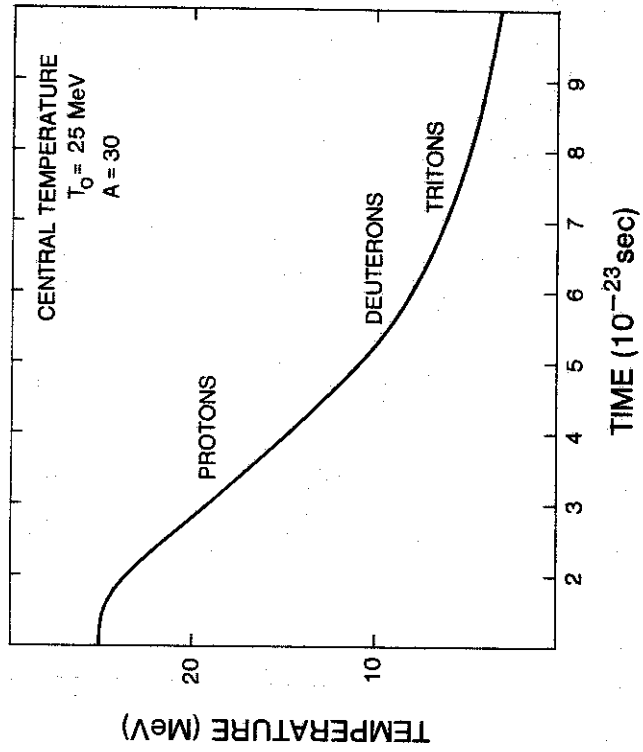


Fig. 5

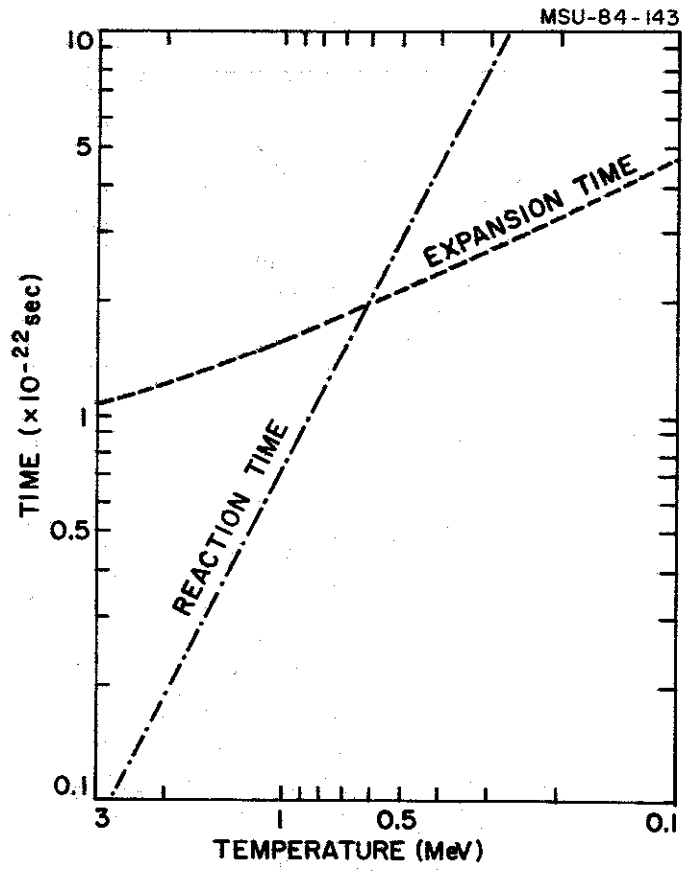


Fig. 6

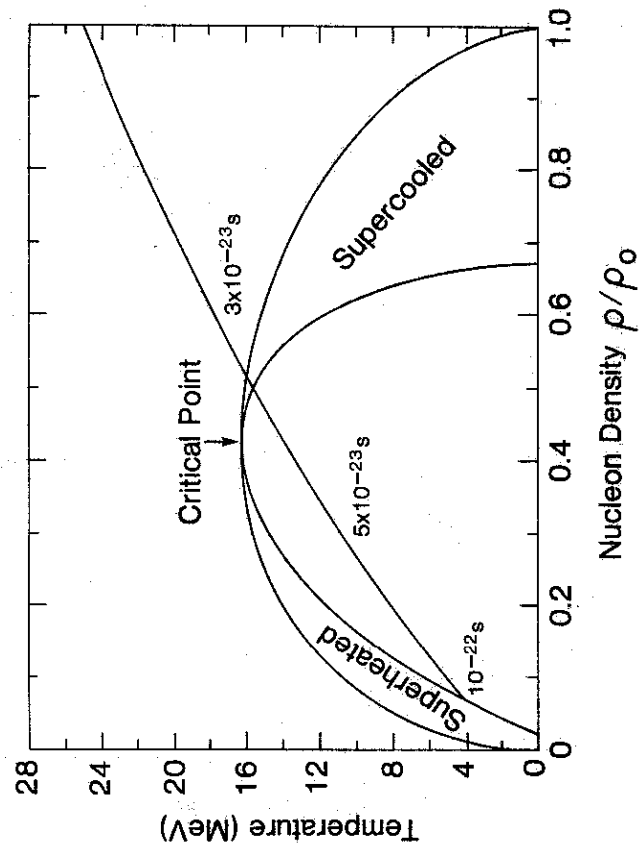
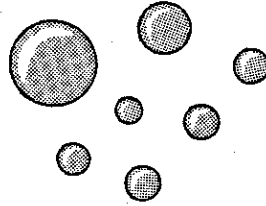
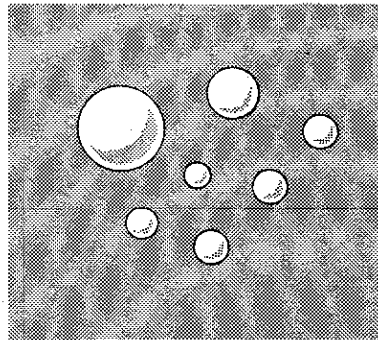


Fig. 7



LOW DENSITIES — DROPLET FORMATION



HIGH DENSITIES — BUBBLE FORMATION

Fig. 8

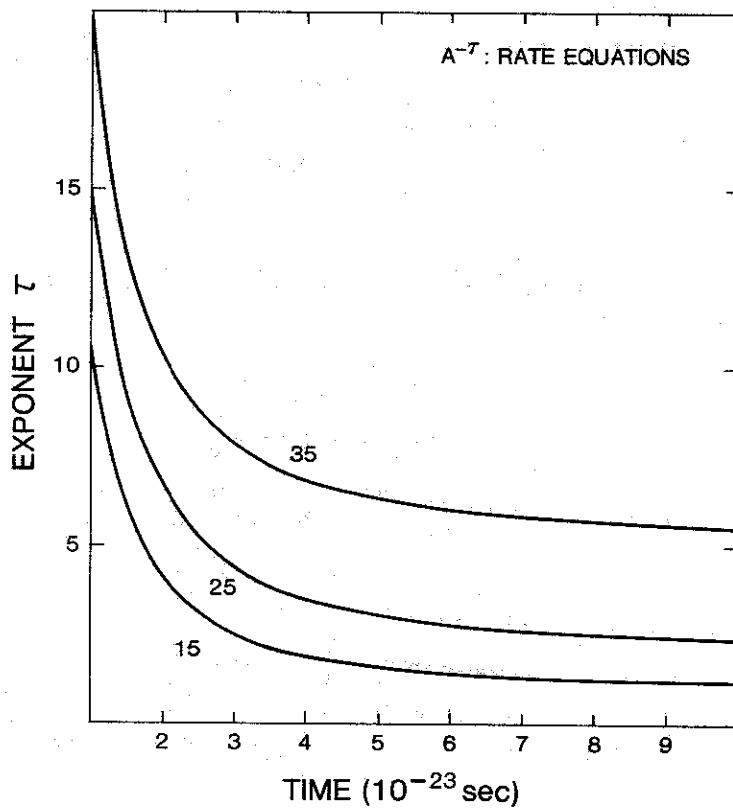


Fig. 9